A remote sensing and GIS based approach for land use/cover, inundation and vulnerability analysis in Moscow, Russia

K. Choudhary [1,4], M.S. Boori [1,2], A.V. Kupriyanov [1,3]
[1] Samara National Research University, 443086, Russia, Samara, Moskovskoye Shosse 34;
[2] American Sentinel University, 2260 South Xanadu Way, Suite 310, Aurora, Colorado 80014, USA;
[3] IPSI RAS - Branch of the FSRC "Crystallography and Photonics" RAS, Molodogvardeyskaya 151, 443001, Samara, Russia;
[4] The Hong Kong Polytechnic University, Hung Hom, Kowloon, Hong Kong

Abstract

Monitoring of land use/cover (LULC) change is very important for sustainable development planning study. This research work is to understand natural and environmental situation and its cause such as intensity, distribution and socio and economic effects in Moscow, Russia based on remote sensing and Geographical Information System techniques. A model was developed by following thematic layers: land use/cover, vegetation, soil, geomorphology and geology in ArcGIS 10.2 software using multi-spectral satellite data obtained from Landsat 7 and 8 for the years of 1995, 2005 and 2016 respectively. Increasing scientific and political interest in regional aspects of global environmental changes, there is a strong stimulus to better understand the patterns causes and environmental consequences of LULC expansion in the elevation of Moscow state, one of the areas in the nation with fast economic growth and high population density. A 70 to 300 m inundation land loss scenarios for surface water and sea level rise (SLR) were developed using digital elevation models of study site topography through remote sensing and GIS techniques by ASTER GDEM and Landsat OLI data. The most severely impacted sectors are expected to be the vegetation, wetland and the natural ecosystem. Improved understanding of the extent and response of SLR will help in preparing for adaptation.

Keywords: LULC, Sea level rise, Landsat data, remote sensing and GIS.

Citation: Choudhary K, Boori MS, Kupriyanov A.V. A remote sensing and GIS based approach for land use/cover, inundation and vulnerability analysis in Moscow, Russia. Computer Optics 2019; 43(1): 90-98. DOI: 10.18287/2412-6179-2019-43-1-90-98.

Acknowledgments: This work was partially supported by the Ministry of education and science of the Russian Federation in the framework of the implementation of the Program of increasing the competitiveness of Samara University among the world's leading scientific and educational centers for 2013-2020 years; by the Russian Foundation for Basic Research grants (# 15-29-03823, # 16-41-630761, # 17-01-00972, # 18-37-00418), in the framework of the state task # 0026-2018-0102 "Optoinformation technologies for obtaining and processing hyperspectral data".

Introduction

Russia has a largely continental climate because of its sheer size and compact configuration. Most of its land is more than 400 km. from the sea and the center is 3,840 km. from the sea. Russia's mountain ranges, predominantly to the south and the east, block moderating temperatures from the Indian and Pacific Oceans but European Russia and northern Siberia lack such topographic protection from the Arctic and North Atlantic Oceans [1, 2]. Moscow located in European Russia. It's the area of high environmental sensitivity zone due to harsh climate conditions with maximum time frozen temperature below than zero. The region is drained by numerous rivers and dotted with lakes due to heavy rainfall. Numerous studies have been performed to understand the variations in the Land surface temperature as a result of changes in the land surface properties [3, 4]. Land use/cover is two fundamentals describing the terrestrial environment in connection with both processes natural and anthropogenic activities.

The unified term land use/cover (LULC) includes both categories of LU and LC and analysis of changes is of prime importance to understand many social and environmental problems [5, 6]. Land use/cover and vulnerability change analysis has emerged as an important research question, because both changes have been identified as a key factor which stands responsible for environmental modification worldwide. Although it is possible to monitor by involving traditional surveys and inventories but Satellite Remote Sensing apart from being advantageous in terms of cost and time saving for regional scale also provides large scale data. Geographic Information Systems (GIS) and Remote Sensing (RS) have proved to be useful tools for assessing the spatiotemporal dynamics [7]. Since the 1960s, scientists have extracted and modeled various vegetation biophysical variables using remote sensing data and the normalized difference vegetation index is one such widely adopted index [8, 9]. An inverse relationship has been reported between land surface temperature and vegetation index.

Nowadays, it is recognized that climate change and sea level rise will impact seriously upon the natural environment and human society in the area [10, 11]. Therefore sea level rise has to be one of the main impacts of climate change in Moscow. Presently remote sensing and GIS techniques are the powerful tools to investigate, predict and forecast environmental change scenario in a reliable,

non-invasive, rapid and cost-effective way with considerable decision-making strategies [12, 13]. The main aim of this research work is to describe natural hazards impacts and land loss due to water level of inundation from 77 to 300 m in Volga river basin located in Moscow.

Study area

Moscow Oblast is a federal subject of Russia (fig. 1). Its population is 7,095120 (2010 census) people living in an area of 44,300 square kilometers. It is one of the most densely populated regions in the country and is the second most populous federal subject. The Oblast has no official administrative center; its public authorities are located in Moscow and across other locations in the Oblast. The latitude of the city is 55° 45’ 7” N and longitude is 37° 36’ 56" E. The region is highly industrialized, such as metallurgy, oil refining, mechanical engineering, food, energy and chemical industries.

The climate of Moscow region is humid continental, short but warm summers and long cold winters. The average temperature is 3.5 °C (38.3 °F) to 5.5 °C (41.9 °F). The coldest months are January and February average temperature of −9 °C (16 °F) in the west and −12 °C (10 °F) in the east. The minimum temperature is −54 °C (−65 °F). Here are more than three hundred rivers in Moscow regions and most rivers belong to the basin of the Volga [14]. Which itself only crosses a small part in the north of Moscow region. They are mostly fed by melting snow and the flood fall on April-May. The water level is low in summer and increases only with heavy rain. The river freezes over from late November until April.

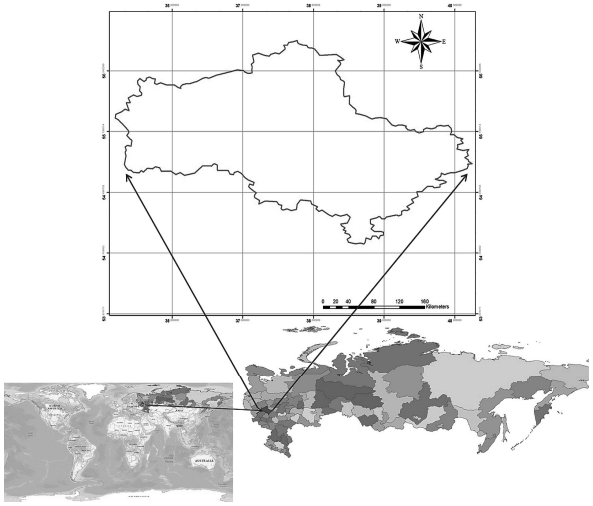

Fig. 1. Location map of the study area in Moscow Region, Russia

Data and methods

In this research work, we used primary data (Satellite data) and secondary data such as ground truth for land use/cover classes and topographic sheets. The ground truth data were collected using Global Positioning System (GPS) for the year 1995 to 2016 in the month of June to September for image analysis and classification accuracy. A selection of multi-sensor, multi-resolution and multi-temporal images was used in this study [15, 16]. The specific satellite images used were Landsat ETM+ (Enhanced Thematic Mapper Plus) for 1995 and 2005, Landsat OLI (Operational Land Imager) for 2016, an image captured by a different type of sensor.

Image pre-processing and classification

In per-processing, first of all three images were georeferenced by WGS 1984 UTM projection [17], later on calibrated and remove three errors. We use specific band combination and use image enhancement techniques such as histogram equalization to improve the classification accuracy. Data sources used for the GCP selection were; digital topographic maps, GPS acquisitions [18, 19]. The data of ground truth were adapted for each single classifier produced by its spectral signatures for producing series of classification maps. For land use classification, supervised maximum likelihood algorithm (MLC) was used in ArcGIS 10.2 software. MLC classification is based on training sites (signature) provided by the analyzer based on his experience or knowledge [20, 21]. After training site, whole image classified according to similar digital value of training site and finally classification give land use/cover classified image of the area [22]. Seven main land cover classes have been found namely agriculture, barren land, forest, settlements, scrubland, waterbody and wetland in the study area (table 1).

Table 1. Classes delineated on the basis of supervised classification

Sr. No.	Class name	Description
1	Agriculture	Cultivated areas, croplands, grasslands, vegetables, fruits etc
2	Barren land	This contains open lands mostly barren but also small vegetation
3	Forest	Small trees and shrub vegetation area except for vegetation
4	Scrubland	Scrub is a plant community describe by vegetation shrubs, often also including grasses and herbs
5	Settlements	Includes construction activities along the coastal dunes as well as sporadic houses within the local village and some governmental buildings
6	Waterbody	All the water within land mainly river, ponds, lakes.etc
7	Wetland	A wetland is a land area with standing water and low soil fertility

Land use/cover change detection

In this research work three date data 1995, 2005 and 2016 were used to identify the changes in the study area. Following the classification of imagery from each individual year, a multi-date, post-classification comparison, change-detection algorithm was used to determine changes during two intervals for 1995-2005 and 2005 to 2016. The post-classification approach provides “from-to” change information which facilitates easy calculation and mapping of the kinds of landscape transformation that have occurred, as shown in figure 2 [23]. Classified image pairs of two different decade data were compared using cross-tabulation in order to determine qualitative and quantitative aspects of the changes for the periods of 1995 to2016, then charts the spatial breakdown of all the land use/cover classes.

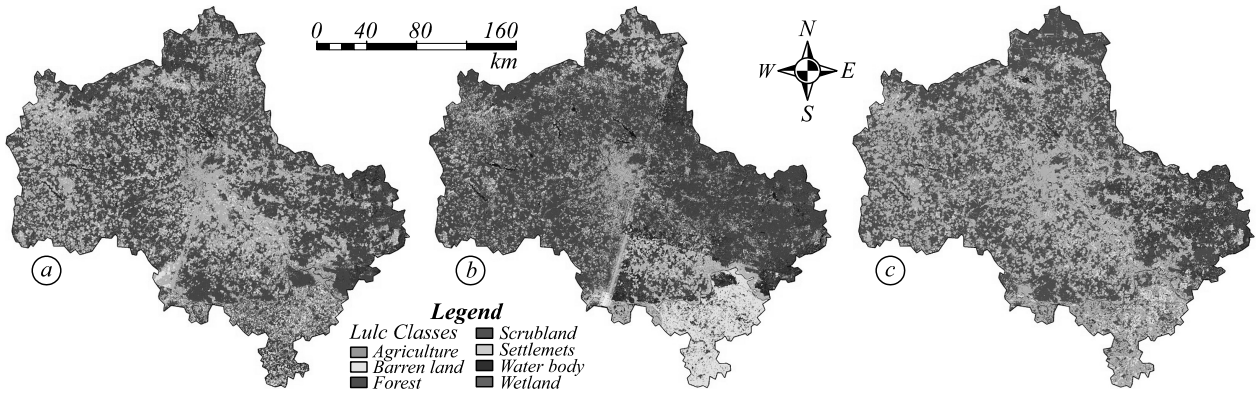

Fig. 2. Land use / cover status of the Moscow Region, Russia: (a) in 1995, (b) in 2005 and (c) in 2016 (based on Landsat ETM+ and OLI Satellite Imagery)

Data analysis

All multi-spectral and temporal data were georeferenced based on topographic sheets with the help of ArcGIS 10.2 software. To improve the quality of research analysis we used different band ratio, image enhancement techniques and principal component analysis and in last supervised classification.

Thematic maps (fig. 3) of geology, geomorphology, soil, vegetation and land use/cover were prepared from Landsat ETM+ and OLI imageries. The weight of all landscape units based on Ecodinamica Tricart 1977 and Barbosa 1997 stability concept, where stability was classified according to table 2. The weights of a landscape unit indicate the importance of any factor in relation to others. In natural vulnerability all thematic layer give the same weight but in environmental vulnerability all thematic layer were given different weight based on their sensitivity in the study area (24-25).

Table 2. Stability values of landscape units. (Ecodinamica Tricart, 1977)

Unit	Pedogenesis / morphogenesis Relation	Value
Stable	Prevails pathogenesis	1.0
Intermediate	Balance between pedogenesis and morphogenesis	2.0
Unstable	Prevails morphogenesis	3.0

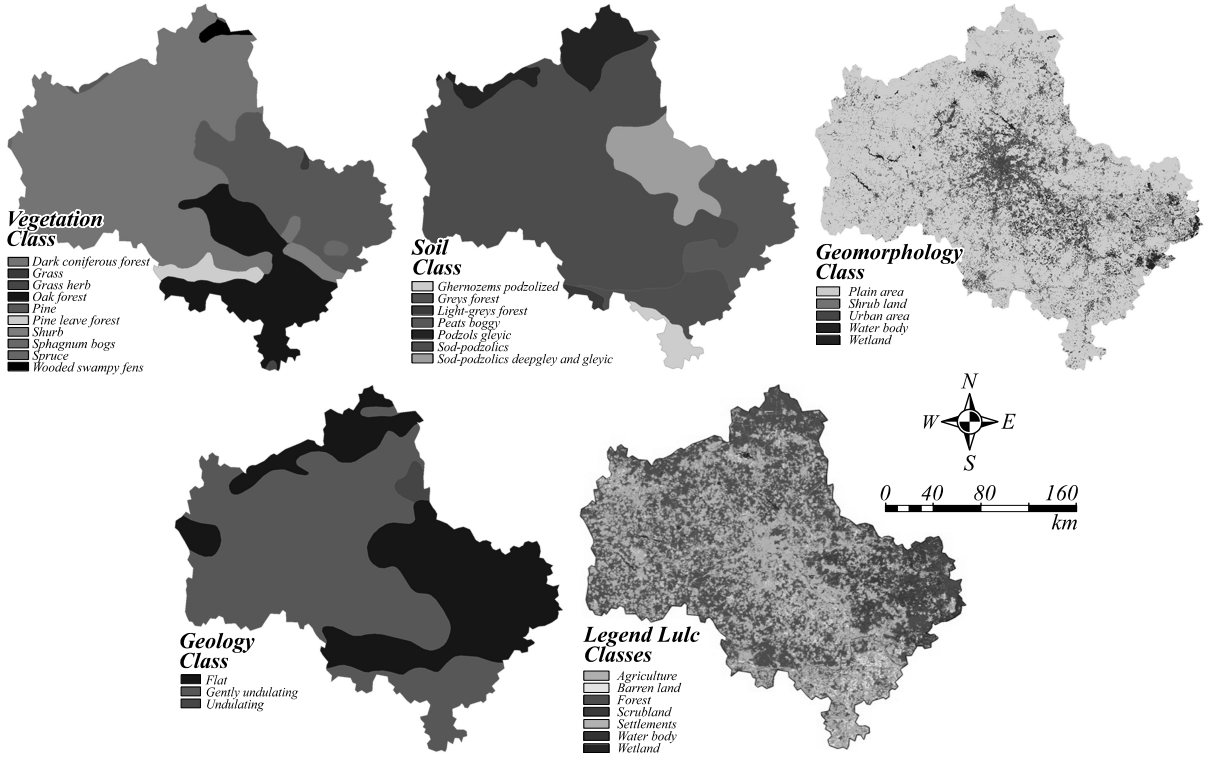

Fig. 3. Simplified vegetation, soil, geomorphology, geology and land use/cover map

The degree of vulnerability for all units was range from 0.0 to 3.0 (table 3) based on Barbosa and Crepani et al. (1996). The degree of vulnerability varies from 0 to 3 and is ranked as an extreme, high, moderate, reasonable and low vulnerability. The weights of compensation indicate the importance of any factor in relation to others, as can be seen in the formula below for natural vulnerability map:

$$[(\text{Theme 1})+(\text{Theme 2})+(\text{Theme 3})+(\text{Theme 4})]/4$$

For environment vulnerability we use following formula:

0.2×[Theme 1] + 0.1×[Theme 2] + 0.1×[Theme 3] + + 0.1×[Theme 4] + 0.5×[Theme 5].

Where:
Theme 1: Geomorphology map,
Theme 2: Simplified geological map,
Theme 3: Soil map,
Theme 4: Vegetation map,
Theme 5: Land use/cover map.

The resulting mean value was distributed in following five natural and environmental vulnerability classes:

1. Low vulnerability: less than or equal to 1.00.
2. Reasonable vulnerability: 1.1 to 1.50.
3. Moderate vulnerability: 1.51 to 2.00.
4. High vulnerability: 2.1 to 2.50.
5. Extreme vulnerability: greater than or equal to 2.51.

Table 3. Weight table for each unite in a thematic layer

Thematic maps/classes	Vulnerability grade levels
Land use/cover	
Agriculture	1.4
Barren land	1
Forest	1.7
Scrubland	2.2
Settlements	3
Waterbody	0.5
Wetland	0.8
Vegetation	
Darkconiferous forest	2.8
Grass	1.9
Grass herb	2
Oak forest	2.7
Pine	2.6
Pine leave forest	2.4
Shrub	2.3
Sphagnum bogs	1.6
Spruce	1.3
Wooded swampy fens	2.9
Geomorphology	
Plain area	2.5
Shrub land	2.3
Urban area	3
Water body	0.5
Wetland	0.8
Geology	
Flat	2.5
Gently undulating	2
Undulating	1.9
Soil	
Chernozems podzolized	1.9
Greys forest	2.1
Light-greys forest	1.8
Peats boggy	1.5
Podzols gleyic	1.4
Sod-podzolics	1.7
Sod-podzolics deep-gley and gleyic	0.9

Inundation analysis

A preparative requirement for the analysis of flooding impacts was the development of spatial datasets [26]. A 1m spatial resolution digital elevation model (DEM) with the error within 224 mm in elevation was constructed using ASTER GDEM images (fig. 4). The GIS environment was used to classify and map the topology of land threatened by inundation. The length of the sand spit at some places is more than 1 km and they are highly vulnerable to river erosion basin.

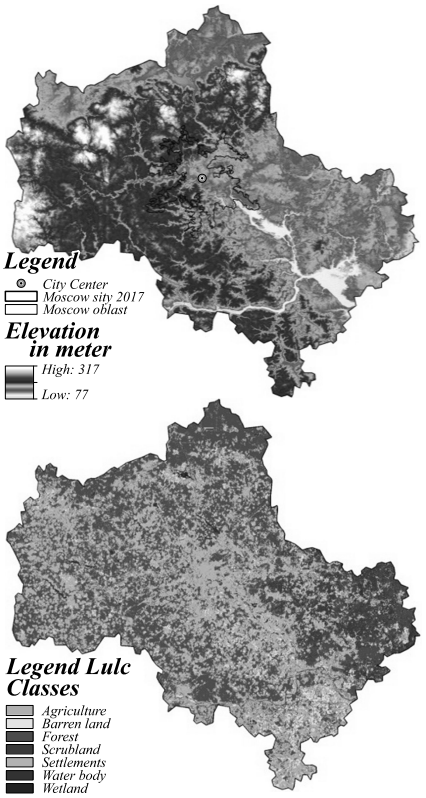

Fig. 4. Elevation and land use/cover map of Moscow, Russia

Results

Land use/cover status

Figure 2 shows land use/cover image supervised classification. These images provide the pattern of land use of the study area. The green color represents agricultural, yellow color barren land, red color forest, gray color settlements, brown color shows the scrubland, blue color shows water body and purple color shows wetland. All land cover class maps were compared with reference data, which was prepared by ground truth, sample points and google earth. Overall classification accuracy of the study area was more than 90 % for all three dates.

Results show that forest area has been most dominant class in the study area for all three dates (fig. 5). Settlements in the study area were less than 2 percent of the total study due to extreme cold and severe climatic conditions. Since 1995 to 2016 water body was little bit variate. These land use/cover change variables from 1995 to 2016 were mainly caused by natural and climatic conditions.

Table 4 shows both positive and negative land use/cover changes in the study area from 1995 to 2005, the major change was in agriculture and forest area. Forest was increased 3,536.13 km^2 (7.56) and agriculture was

decreased 7169.51 km^2 (15.33%) of the total study area due to hares climatic conditions. From 2005 to 2016 total agriculture area was increased from 6,899.62 km^2. In the same time period other classes such as barren land, scrubland, settlements, water body and wetland increase respectively. From 2005 to 2016 total agriculture area was increased from 6,899.62 km^2 and other classes' settlements and water body were increased.

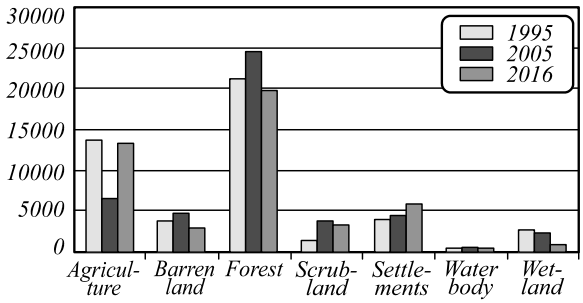

Fig. 5. Land use/cover for Moscow Region, Russia in 1995, 2005 and 2016

The results show that from 1995 to 2005, 3820.91 km^2 agriculture areas were stable but 990.98 km^2 areas converted from forest to agriculture (table 5). In the same time period 15982.20 km^2 forest areas was stable but 1662.39 km^2 wetland area was encroached by forest. Maximum stable class was water body, where 293.26 km^2 areas were stable from 1995 to 2005. In second half from 2005 to 2016 3926.40 km^2 agriculture areas was stable and 2711.65 km^2 barren land, 4401.14 km^2 forest and 1129.97 km^2 scrubland area converted into agriculture land due to the increase of market demand. In this time period there is a not a big change in wetland and maximum bare land area 276.12 km^2 was stable. Scrubland 906.20 km^2 and wetland 1238.38 km^2 area was converted into forest area which shows governmental protection from 2005 to 2016. Since 2005 to 2016, 2354.45 km^2 settlements area was stable but 1798.50 km^2 forest area was converted into settlements. In the second half again water body area was highly stable area around 326.62 km^2.

Table 4. Area and amount of change in different land use categories in the study area from 1995 to 2016

Class	1995		2005		2016	
	Area Km^2	%	Area Km^2	%	Area Km^2	%
Agriculture	13673.51	29.24	6504.00	13.91	13403.62	28.66
Barrenland	3802.63	8.13	4717.74	10.09	2993.18	6.40
Forest	21135.18	45.19	24671.31	52.75	19896.64	42.54
Scrubland	1268.97	2.71	3791.82	8.11	3377.49	7.22
Settlements	3898.31	8.34	4361.75	9.33	5852.00	12.51
Waterbody	408.96	0.87	430.13	0.92	449.45	0.96
Wetland	2580.57	5.52	2291.37	4.90	795.75	1.70
Total	46768.12	100.00	46768.12	100.00	46768.12	100.0

Table 5. Land use/cover change matrix showing land encroachment of the study area

CLASS 1995-2005	**Agriculture**	**Barrenland**	**Forest**	**Scrubland**	**Settlement**	**Waterbody**	**Wetland**	**Total**
Agriculture	3820.91	2119.56	4633.85	1396.83	1318.99	15.29	503.14	13808.57
Barrenland	867.28	1091.05	910.37	215.43	522.59	1.39	127.87	3735.99
Forest	990.98	583.75	15982.20	1517.75	605.99	44.48	1384.32	21109.46
Scrubland	198.75	244.62	365.54	205.70	82.00	20.85	125.09	1242.55
Settlements	458.66	276.59	1178.62	198.75	1599.75	13.90	151.50	3877.76
Waterbody	8.34	4.17	41.70	22.24	40.31	293.26	2.78	412.79
Wetland	150.11	418.35	1662.29	137.60	122.31	2.78	87.56	2581.00
Total	6495.04	4738.09	24774.56	3694.29	4291.94	391.95	2382.25	46768.12
CLASS 2005-2016	**Agriculture**	**Barrenland**	**Forest**	**Scrubland**	**Settlement**	**Waterbody**	**Wetland**	**Total**
Agriculture	3926.40	622.67	1067.43	137.60	717.18	1.39	40.31	6512.97
Barrenland	2711.65	964.57	414.18	27.80	528.15	2.78	88.95	4738.09
Forest	4401.14	480.16	15697.28	2155.70	1798.50	41.70	69.49	24643.96
Scrubland	1129.97	500.88	906.20	915.93	300.21	38.92	29.19	3821.29
Settlements	1099.39	291.30	451.71	43.09	2354.45	27.53	45.87	4313.33
Waterbody	59.75	0.00	16.68	11.12	36.14	326.62	0.00	450.30
Wetland	220.88	116.75	1238.38	193.19	230.72	12.13	276.12	2288.17
Total	13549.18	2976.32	19791.85	3484.42	5965.35	451.06	549.92	46768.12

Vulnerability analysis

Natural and environmental vulnerability maps are shown the relationship in between landscape and vulnerability and able to tackle answers such as comparing different types of vulnerability zones in the study area.

Natural vulnerability

Its map shows that maximum area in safe zones as 56.91 % area in moderate vulnerability and 20.10 % area in reasonable vulnerability zones, which represent that around 78 % area of the total study area is the safe zone. Around 11.70 % area goes in high vulnerability which is really need proper management otherwise it will increase and harmful. The low vulnerability area is only 5.44 % of the total study area, which is present in river and water body area. 5.83 % area has been under extreme vulnerability, which is very less and close to water bodies. High vulnerability is due to fluctuation and

extreme climate condition. Maximum vegetation area and close to river basin area under moderate vulnerability zone. Some part of wetland and vegetation under reasonable vulnerability and low vulnerability area, which represent maximum safe area in this study area. It is low vulnerability area due to less socio-economic activities and high density of vegetation (fig. 6).

Environmental vulnerability

Environmental vulnerability map is more sensitive than natural vulnerability. In environmental vulnerability around 46 % area under moderate vulnerability zone but high and extreme vulnerability is higher than natural vulnerability. Here 7.23 % area under high vulnerability and 9.83 % under extreme vulnerability. Reasonable vulnerability is 36.13 % and low vulnerability is 1.58 %. Low vulnerability is present in river and water bodies, reasonable vulnerability present in wasteland and some parts in vegetation. Maximum study area has been under moderate vulnerability, which is present in vegetation and close to wetland and coastal line. High vulnerability is present in close to river and its channels (fig. 6).

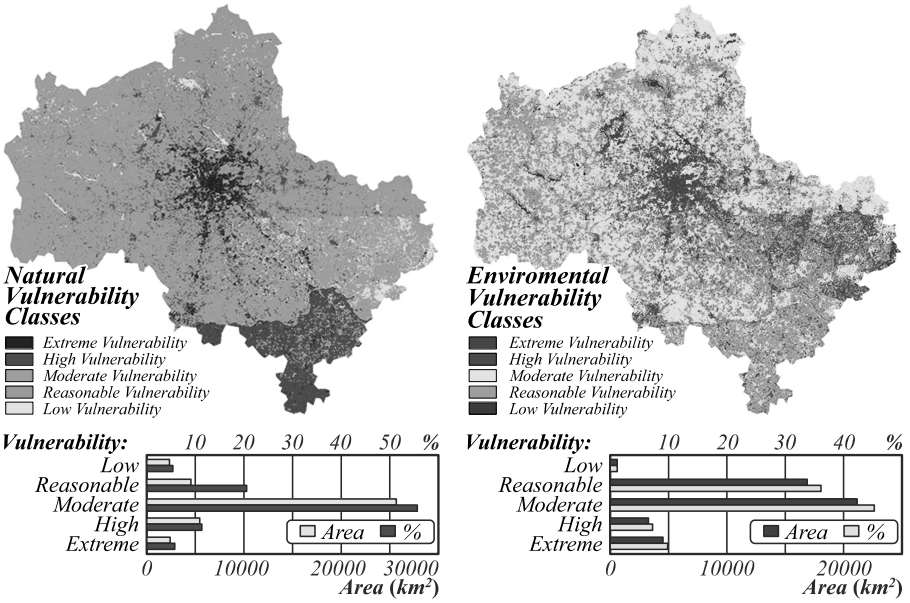

Fig. 6. Natural and environmental vulnerability map

As study area is in the north part of the Asia so maximum time of the year it is cover with ice, with harsh climatic condition. In winter only airways are the only way of approaching this area but in Summer Rivers also provide transportation facility. Here land use / cover classes and there convergent or encroachment induced by extreme cold and tough climatic condition in the study area. In extreme cold condition maximum areas convert in wasteland, where land has been unfertile. But in summer session ice has been melt and maximum land convert into wetland, forest and vegetation area etc.

Land loss due to inundation

The DEM presented in figure 7 shows that low-lying land is more extensive at the north and center of the study area. The areas lower than 1m above mean sea level (MSL), which are at risk of inundation under the minimum inundation level are vegetation, industry and urban area basically the whole city.

The main results of land loss due to inundation are presented in Figure 8. The most significant changes would occur south-east side of the Moscow.

At the minimum inundation level (70 m in fig. 8), 0.04 % (20.24 km^2) of the total area (table 6) would be flooded including: urban areas, natural vegetation and agricultural land and beaches.

The area of submergence for 80 m rise in water level is up to 60.12 km^2 (0.13 %) and subsequently for 90 m 258.29 km^2 (0.55 %), 100 m 895.84 km^2 (1.92 %), 110 m 2417.18 km^2 (5.18 %), 120 m 5108.59 km^2 (10.94 %), 130 m 8779.34 km^2 (18.80), 140 m 12815.38 km^2 (27.44 %), 150 m 16792.16 km^2 (35.95 %), 180 m 27976.67 km^2 (59.88 %), 210 m 38787.89 km^2 (82.98 %), 240 m 44584.13 km^2 (95.37 %), 275 m 46578.68 km^2 (99.62 %) and 300 m 46754.70 km^2 (100 %) respectively (table 6). From the land use/cover map, it is clear that the maximum area is covered by agriculture which includes Moscow city. At the full inundation level 300m in fig. Such a loss of land implies that the population living presently in these areas would be displaced. Even if some parts of the ecosystem of the wetland are not destroyed, because those parts could adapt to sea level rise and move landwards, the species richness is likely to decrease, due to repugnant new conditions where several plant communities and rare species would disappear. The area least vulnerable to inundation would be the southern and east part of the study area. However, parts of city and port, as well as an important river beach and natural forest would be flooded.

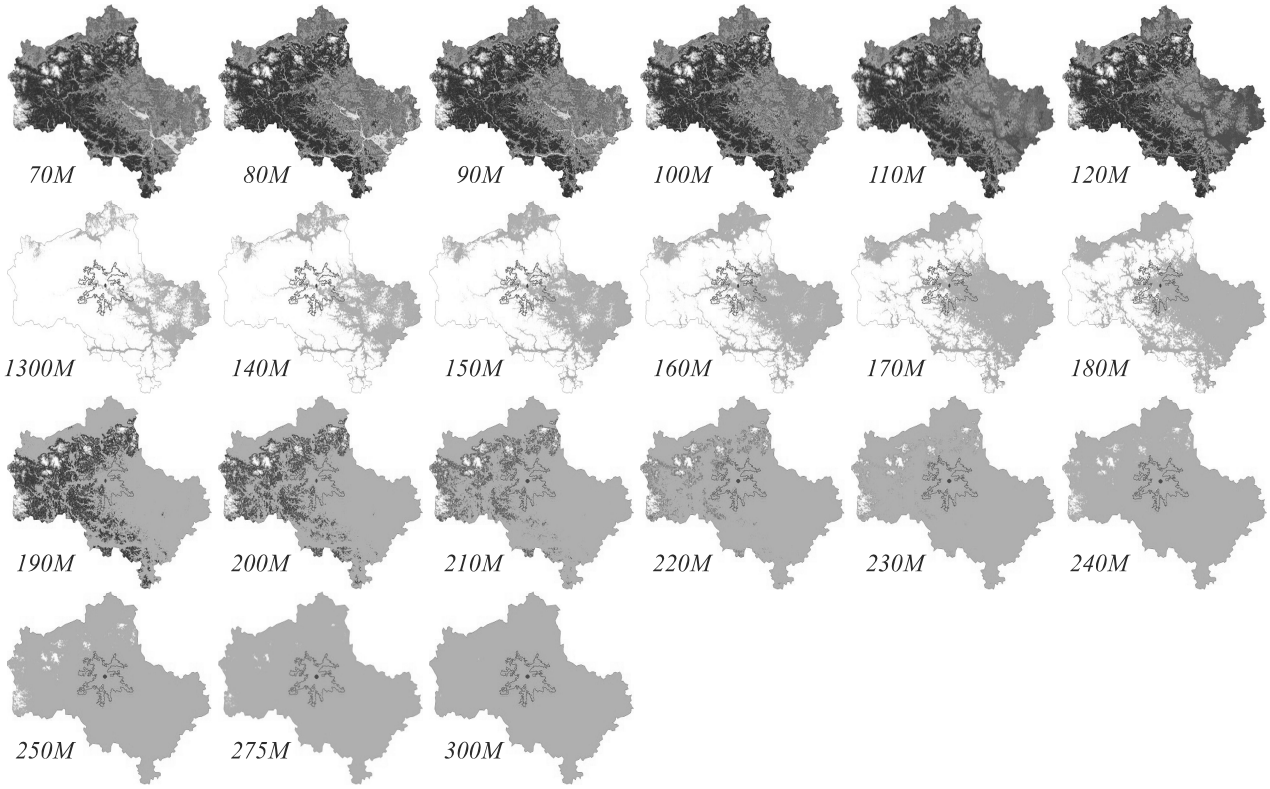

Fig. 7. Land areas vulnerable to inundation in the Moscow, Russia

Table 6. Potential land loss of the main sectors for 70 m to 300 m inundation levels scenarios (in km² and in % of the total inundated areas)

Class name	70M		80M		90M		100M		110M		120M		130M	
	km²	%	km²	%	km²	%	km²	%	km²	%	km²	%	km²	%
Agriculture	4.92	24.32	22.86	38.02	119.46	46.25	388.84	43.41	853.78	35.32	1581.83	30.96	2557.14	29.13
Barrenland	2.35	11.62	6.56	10.91	27.79	10.76	99.96	11.16	285.46	11.81	564.95	11.06	866.86	9.87
Forest	3.38	16.68	9.33	15.52	37.41	14.48	123.66	13.80	364.95	15.10	1001.52	19.60	2184.16	24.88
Scrubland	6.18	30.54	12.33	20.51	39.49	15.29	157.59	17.59	549.33	22.73	1182.53	23.15	1812.09	20.64
Settlements	1.66	8.18	4.23	7.04	16.80	6.50	71.10	7.94	229.20	9.48	542.06	10.61	1031.46	11.75
Waterbody	1.30	6.41	3.69	6.14	12.58	4.87	36.90	4.12	90.60	3.75	143.23	2.80	186.29	2.12
Wetland	0.45	2.24	1.12	1.86	4.76	1.84	17.79	1.99	43.85	1.81	92.48	1.81	141.34	1.61
Total	20.24	0.04	60.12	0.13	258.29	0.55	895.84	1.92	2417.18	5.18	5108.59	10.94	8779.34	18.80
Class name	**140M**		**150M**		**160M**		**170M**		**180M**		**190M**		**200M**	
	km²	%	km²	%	km²	%	km²	%	km²	%	km²	%	km²	%
Agriculture	3605.91	28.14	4651.49	27.70	5722.11	27.79	6903.08	28.39	8202.99	29.32	9545.05	30.03	10772.92	30.31
Barrenland	1159.12	9.04	1448.88	8.63	1724.89	8.38	2000.08	8.23	2266.48	8.10	2506.25	7.88	2689.91	7.57
Forest	3667.29	28.62	5188.49	30.90	6621.71	32.16	7975.34	32.80	9352.34	33.43	10959.28	34.48	12840.17	36.13
Scrubland	2363.85	18.45	2793.90	16.64	3072.01	14.92	3225.66	13.27	3291.92	11.77	3317.75	10.44	3332.07	9.38
Settlements	1627.70	12.70	2272.80	13.53	2939.31	14.27	3611.60	14.85	4225.56	15.10	4780.97	15.04	5198.22	14.63
Waterbody	219.43	1.71	240.84	1.43	299.20	1.45	370.93	1.53	394.77	1.41	418.45	1.32	431.27	1.21
Wetland	172.08	1.34	195.77	1.17	213.47	1.04	227.91	0.94	242.61	0.87	258.15	0.81	273.61	0.77
Total	12815.38	27.44	16792.16	35.95	20592.70	44.08	24314.60	52.05	27976.67	59.88	31785.89	68.02	35538.18	76.04
Class name	**210M**		**220M**		**230M**		**240M**		**250M**		**275M**		**300M**	
	km²	%	km²	%	km²	%	km²	%	km²	%	km²	%	km²	%
Agriculture	11770.03	30.34	12506.84	30.26	13040.38	30.16	13413.83	30.09	13655.11	30.01	13881.56	29.80	13902.42	29.73
Barrenland	2813.50	7.25	2886.41	6.98	2933.22	6.78	2962.56	6.64	2980.15	6.55	2992.10	6.42	2992.955	6.40
Forest	14680.51	37.85	16235.11	39.28	17450.69	40.37	18331.89	41.12	18951.63	41.64	19740.06	42.38	19889.92	42.54
Scrubland	3342.19	8.62	3350.29	8.11	3357.22	7.77	3362.99	7.54	3368.20	7.40	3376.74	7.25	3377.19	7.22
Settlements	5459.78	14.08	5620.17	13.60	5716.00	13.22	5776.87	12.96	5815.11	12.78	5847.92	12.55	5851.71	12.52
Waterbody	437.79	1.13	441.77	1.07	444.10	1.03	445.60	1.00	446.68	0.98	449.23	0.96	449.42	0.96
Wetland	284.08	0.73	287.53	0.70	289.38	0.67	290.39	0.65	290.77	0.64	291.07	0.62	291.09	0.62
Total	38787.89	82.98	41328.12	88.41	43230.99	92.48	44584.13	95.37	45507.66	97.34	46578.68	99.62	46754	100.00

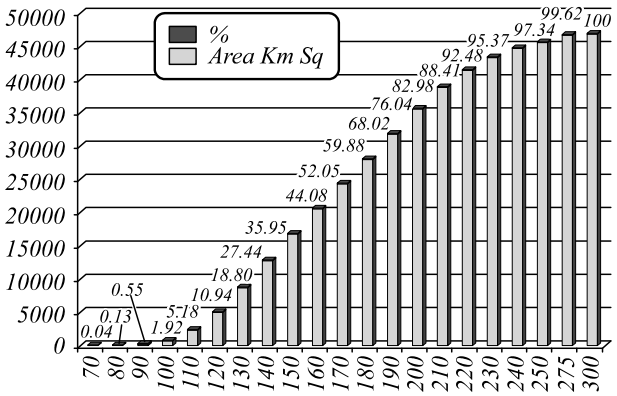

Fig. 8. Inundation area graph of the Moscow, Russia

Conclusion

This study shows the importance of land use / cover change detection, vulnerability and inundation assessment for resource management, planning and sustainable development. Results of this research work is helpful for proper utilization of land, there accurate strategical development and conversion in specific timeframe. Here Remote Sensing and GIS data provide extensive opportunity for this type of land use change study, which is not possible with conventional methods in impassable area. Based on multi-temporal Landsat images, we determined that there was significant expansion of anthropogenic land cover in the Moscow. Analysis revealed that the area of anthropogenic land cover was increased, resulting in a substantial reduction in natural land cover. Land use/cover change and vulnerability scenarios are useful for exploring uncertainties in vulnerability assessment on a regional basis, some regions show equal vulnerability to all scenarios, while other regions show different responses. The inundation maps can be overlaid on land use/cover maps to find out the extent of submergence of different land use/cover areas. By contrast, arable land declined by 10% due to occupation by urbanization and industrialization. It is necessary to incorporate the elevation levels for new settlements areas under the town planning acts so that human life and property are saved from natural hazards. The run-up levels can be used as guidance to determine safe locations of settlements from river basin. This is an indicator of where we can be more or less uncertain about the future. Furthermore, it helps in indicating how society and policy can have an important role to play in future development pathways. The mapping, monitoring and modeling of land use/cover in such a vast territory as Moscow region could also contribute to the study of global environmental change.

References

[1] Amiri F, Rahdari V, Najafabadi SM, Pradhan B, Tabatabaei T. Multi-temporal Landsat images based on eco-environmental change analysis in and around Chah Nimeh reservoir, Balochestan (Iran). Environmental Earth Sciences 2014; 72(3): 801-809. DOI: 10.1007/s12665-013-3004-9.

[2] Bai J, Chen X, Yang L, Fang H. Monitoring variations of inland lakes in the arid region of Central Asia. Frontiers of Earth Science 2012; 6(2): 147-156. DOI: 10.1007/s11707-012-0316-0.

[3] Choudhary K, Boori MS, Kupriyanov A. Spatial modelling for natural and environmental vulnerability through remote sensing and GIS in Astrakhan, Russia. Egypt J Remote Sensing Space Sci 2017; 21(2): 139-147. DOI: 10.1016/j.ejrs.2017.05.003.

[4] Barbosa CCF. Álgebra de mapas e suas aplicações em Sensoriamento Remoto e Geoprocessamento. Dissertação (Mestrado em Sensoriamento Remoto). Instituto Nacional de Pesquisas Espaciais (INPE), São José dos Campos, 1997.

[5] Cui L, Ge Z, Yuan L, Zhang L. Vulnerability assessment of the coastal wetlands in the Yangtze Estuary, China to sea-level rise. Estuarine, Coastal and Shelf Science 2015; 156: 42-51. DOI: 10.1016/j.ecss.2014.06.015.

[6] Sweet WV, Park J. From the extreme to the mean: Acceleration and tipping points of coastal inundation from sea level rise. Earth's Future 2014; 2(12): 579-600. DOI: 10.1002/2014EF000272.

[7] Yabuki H, Park H, Kawamoto H, Suzuki R, Razuvaev VN, Bulygina ON, Ohata T. Baseline Meteorological Data in Siberia (BMDS). Version 5.0, RIGC, JAMSTEC, Yokosuka, Japan, Distributed by CrDAP, Digital Media 2011. Source: ⟨https://ads.nipr.ac.jp/kiwa/Graph.action?owner_site=ADS&fileIdentifier=A20131107-002&version=5.00#⟩.

[8] Choudhary K, Boori MS, Kupriyanov A. Landscape analysis through remote sensing and GIS techniques: a case study of Astrakhan, Russia. Proc SPIE 2017; 10225: 102251U. DOI: 10.1117/12.2266245.

[9] Grigio AM, De Castro AF, Souto MVS, Amaro VE, Vital H, Diodato MA. Use of remote sensing and geographical information system in the determination of the natural and environmental vulnerability of the Guamaré municipal district – Rio Grande do Norte – northeast of Brazil. Journal of Coastal Research 2004; III(SI 39): 1427-1431.

[10] Choudhary K, Boori MS, Kupriyanov AV. Mapping and evaluating urban density patterns in Moscow, Russia. Computer Optics 2017; 41(4): 528-534. DOI: 10.18287/2412-6179-2017-41-4-528-534

[11] Padgett J, Tapia C. Sustainability of natural hazard risk mitigation: Life cycle analysis of environmental indicators for bridge infrastructure. J Infrastruct Syst 2013; 19(4): 395-408. DOI: 10.1061/(ASCE)IS.1943-555X.0000138.

[12] Romero AF, Abessa DMS, Fontes RFC, Silva HG. Integrated assessment for establishing an oil environmental vulnerability map: Case study for the Santos Basin region, Brazil. Marine Pollution Bulletin 2013; 74(1): 156-164. DOI: 10.1016/j.marpolbul.2013.07.012.

[13] Nigel R, Rughooputh SDDV. Soil erosion risk mapping with new datasets: an improved identification and prioritization of high erosion risk areas. Catena 2010; 82(3): 191-205. DOI: 10.1016/j.catena.2010.06.005.

[14] Thakur AK, Sing S, Roy PS. Orthorectification of IRS-P6 LISS IV data using Landsat ETM+ and SRTM datasets in the Himalayas of Chamoli district, Uttarakhand. Curr Sci 2008; 95(10): 1458-1463.

[15] Courchamp F, Hoffmann BD, Russell JC, Leclerc C, Bellard C. Climate change, sea-level rise, and conservation: keeping island biodiversity afloat. Trends in Ecology and Evolution 2014; 29(3): 127-130. DOI: 10.1016/j.tree.2014.01.001.

[16] Yuan F, Sawaya KE, Loeffelholz BC, Bauer ME. Land cover classification and change analysis of the Twin Cities (Minnesota) metropolitan area by multitemporal Landsat

remote sensing. Remote Sens Environ 2005; 98(2-3): 317-328. DOI: 10.1016/j.rse.2005.08.006.
[17] Saboori B, Sulaiman J, Mohd S. Economic growth and CO2 emission in Malaysia: A cointegration analysis of the Environmental Kuznets Curve. Energy Policy 2012; 51: 184-191. DOI: 10.1016/j.enpol.2012.08.065.
[18] Mendoza ME, Granados EL, Geneletti D, Pérez-Salicrup DR, Salinas V. Analysing land cover and land use change processes at watershed level: a multitemporal study in the Lake Cuitzeo Watershed, Mexico (1975-2003). Appl Geogr 2010; 31(1): 237-250. DOI: 10.1016/j.apgeog.2010.05.010.
[19] Stefanov WL, Ramsey MS, Christensen PR. Monitoring urban land cover change: an expert system approach to land cover classification of semiarid to arid urban centers. Remote Sens Environ 2001; 77(2): 173-185.
[20] Thinh NX. Contemporary spatial analysis and simulation of the settlement development of the Dresden city region. 17th International Conference Informatics for Environmental Protection 2003: 253-261.
[21] Thinh NX, Arlt G, Heber B, Hennersdorf J, Lehmann I. Pin-pointing sustainable urban land-use structures with the aid of GIS and cluster analysis. In Book: Hilty LM, Gilgen PW, eds. Sustainability in the information society, 15th symposium informatics for environmental protection, metropolis. Marburg: Metropolis Verlag; 2013: 559-567.
[22] Weng QH. Land use change analysis in the Zhujiang Delta of China using satellite remote sensing, GIS and stochastic modelling. Journal of Environmental Management 2002; 64(3): 273-284. DOI: 10.1006/jema.2001.0509.
[23] Wilson EH, Hurd JD, Civco DL, Prisloe MP, Arnold C. Development of a geospatial model to quantify, describe and map urban growth. Remote Sens Environ 2003; 86(3): 275-285. DOI: 10.1016/S0034-4257(03)00074-9.
[24] Saaty TL. The analytic hierarchy process: Planning, priority setting, resource allocation. New York: McGraw Hill; 1980. ISBN: 978-0-07-054371-3.
[25] Wu KY, Ye ZY, Qi ZF, Zhang H. Impacts of land use/land cover change and socioeconomic development on regional ecosystem services: The case of fast-growing Hangzhou metropolitan area, China. Cities 2013; 31: 276-284. DOI: 10.1016/j.cities.2012.08.003.
Yagoub M. Monitoring of urban growth of a desert city through remote sensing: Al-Ain, UAE, between 1976 and 2000. International Journal of Remote Sensing 2004; 25(6): 1063-1076. DOI: 10.1080/0143116031000156792.

Authors' information

Komal Choudhary has completed her Bachelors and Master's degree in Geography from University of Rajasthan, India in the year 2003 and 2005 respectively. She also completed Bachelors of education in 2007 from University of Rajasthan, India. She has more than 50 international publications including books on vulnerability, risk assessment and climate change. Her prime research interest is "Sustainable Development Studies through Multi-Criteria Approach". After her education she was a college level lecturer in Indian college and she has to her credit an illustrious experience in teaching and other administrative responsibilities spanning over a decade and has served in various capacities like Principal, Faculty Development and Controller of Examinations. Komal brings with herself a vast experience in curriculum design, research guidance and innovative teaching. She visited Brazil, USA, Europe, Russia, India and Hong Kong. E-mail: *komal.kc06@gmail.com* .

Prof. Dr. Mukesh Singh Boori (b. 1980) is Senior Scientist in Samara University, Russia, and Adjunct Professor in American Sentinel University, Colorado, USA. Currently he is involved in remote sensing and GIS teaching and Russian academic excellence project. He has also held positions at University of Bonn Germany, Hokkaido University Japan, Palacky University Czech Republic, Ruhr University Bochum Germany, Leicester University UK, NOAA/NASA USA, JECRC University, JKLU University, MDS University and JSAC/ISRO India. He hold Postdoc from University of Maryland USA, PhD from Federal University – RN (UFRN) Brazil, Predoc from Katholiek University Leuven Belgium, MSc from MDS University and BSc from University of Rajasthan India. He received several distinguish awards including national academy of sciences (NAS) fellowship through national research council (NRC) central government of USA Washington DC, European union social fund through ministry of education, youth & sports Czech Republic, Honorary fellow University of Leicester UK, Prestigious Brazil-Italy government fellowship, Belgian and Indian government space fellowship. He published 100+ peer-reviewed papers including books as a first author in the field of earth and space science and his prime research interest is satellite earth observations through remote sensing & GIS technology. He is a member of many scientific societies / journals / committees, led a number of projects, organized a number of conferences, delivered conference opening ceremony speech, invited talk, chaired sessions and visited 21 countries. E-mail: *msboori@gmail.com* .

Prof. Alexander Victorovich Kupriyanov (born 1978) graduated with honors from Samara State Aerospace University (SSAU) (2001). Candidate's degree in Technical Sciences (2004) and Doctor of Engineering Science (2013). Currently, Senior Researcher at the Image Processing Systems Institute, Russian Academy of Sciences, and part-time position as Associate Professor at SSAU's Technical Cybernetics sub-department. Areas of interest: digital signals and image processing, pattern recognition and artificial intelligence, nanoscale image analysis and understanding, biomedical imaging and analysis. More than 90 scientific papers, including 42 published articles and 2 monographs. E-mail: *ak-upr@smr.ru* .

Received July 17, 2018. The final version – November 11, 2018.